Future Technology
Open Access Journal
ISSN 2832-0379

May 2026| Volume 05 | Issue 02 | Pages 228-240

Journal homepage: https://fupubco.com/futech

https://doi.org/10.55670/fpll.futech.5.2.22

Future Publishing LLC

Article

AI-driven assessment of urban greenway restorative environments: integrating deep learning, street view imagery, and environmental psychology

Xueyan Jing*, Mohd Fabian Hasna, Aini Jasmin Ghazalli

Faculty of Design and Architecture, Universiti Putra Malaysia, 43400 Serdang, Selangor, Malaysia

ARTICLE INFO

Article history:
Received 21 October 2025
Received in revised form
12 February 2026
Accepted 11 March 2026

Keywords:
Urban greenway, Restorative environment, Deep learning, Street view image, Attention recovery theory

*Corresponding author
Email address:
gs64663@student.upm.edu.my

DOI: 10.55670/fpll.futech.5.2.22

ABSTRACT

Existing methods for evaluating urban greenway restorative environments lack objectivity, efficiency, and theoretical integration. The purpose of this research is to develop a restorative environmental assessment framework for urban road binding using deep learning, street-view image data, and environmental psychology theory. It uses a semantic segmentation model called DeepLabV3+ to collect six visual environment features which are otherwise difficult to represent numerically. At the same time, it offers a methodological path for the interdisciplinary integration of artificial intelligence technology and environmental psychology theory. The calculation model of the comprehensive recovery index is constructed in four dimensions based on attention recovery theory. According to empirical analysis, this framework can successfully identify systematic differences in the restorative dimension of different types of binding paths. The presence of greenness can make a large positive contribution to the restorative effect, while building occlusions can have an inhibitory effect. The evaluation results are quite consistent with theoretical predictions and have good robustness in parameter Settings. The findings of the study offer a scientific evaluation tool for accurate diagnosis and optimization improvement of the urban road binding restorative environment. At the same time, it offers a methodological path for the interdisciplinary integration of artificial intelligence technology and environmental psychology theory.

1. Introduction

Greenways are linear corridor systems made up of urban green Spaces with close connections facilitated by possible systems. They can help residents with their physical and mental health. The occurrence of sedentary behavior has been significantly reduced by exposure to greenways, as large-scale natural experiments have shown [1]. Systematic reviews and meta-analyses have confirmed that greenway interventions have a robust positive effect on physical activity levels [2]. Research on greenway location optimization based on individual travel assessment indicates that a scientifically planned greenway network can promote active traffic travel [3], while the structural equation model analysis of community greenway usage behavior reveals multi-level factors influencing greenway utilization [4]. It is also worth noting the positive impact of urban green Spaces on mental health, in addition to their promoting effect on physical activity. Empirical studies have shown that small and medium-sized Green Spaces (GPP) enhance suburban residents' psychological well-being [5]. The synergistic effect of bio-affinity design elements and perceived naturalness enhances the subjective vitality of green Spaces [6,7], while the development of street-view imaging technology has opened a new path for fine-scale research on urban environments [8]. Although the health benefits of urban greenways have been widely recognized, the existing assessment methods still face challenges - traditional remote sensing technology is difficult to capture the greenery perception in pedestrians' actual visual experience, the questionnaire survey method is limited by sample size and subjective bias, and the expert evaluation method faces the predicament of efficiency and standardization. These methodological limitations have prompted the academic community to explore more objective and efficient approaches to greenway environmental assessment. The technology that analyzes street views using deep learning may offer a possible solution to the issue mentioned above. Semantic segmentation methods for urban greening

measurement have formed a relatively complete technical system [9]. Deep learning, combined with street-view imagery, has enabled fine-grained measurement of green structure [10], with neural networks demonstrating improved performance in street-view greening assessment [11]. The amalgamation of multi-source remote sensing imagery along with deep learning has broadened the data sources for street greening monitoring [12]. The development of generative AI technologies provides new directions for visual language assessment of street scenarios [13]. Deep learning and 3D reconstruction technology have enabled multifaceted dynamic analysis of urban vegetation landscapes [14]. Scene semantic analysis has systematically examined human perception measurement of street scenarios [15]. The use of convolutional neural networks for recognizing visual features of urban street vitality demonstrates the effectiveness of deep learning for the complex scene-understanding task in the application [16]. Urban environmental visual features can be automatically extracted at a large scale with these technologies. Nevertheless, existing research mainly focuses on calculating individual indicators such as green vision rate and lacks a systematic evaluation framework that covers multi-dimensional environmental features and their psychological-perceptual human aspects.

The study has systematically examined the core essence of the attention recovery theory and clearly demonstrated that the four dimensions of distance perception, attractiveness, extensibility, and compatibility have key guiding significance for the design of restorative environments [17]. Research through meta-analysis has found group differences in restorative value according to nature [18]. The theoretical model of a restorative urban environment from the perspective of healthy cities provides an integrated analytical framework for studying restorative experience in urban built environments [19]. Research on the contribution of exposure to urban green space to stress and attention recovery verified the applicability of attention recovery theory in specific spatial contexts [20]. Virtual reality technology provides controllable experimental means for restorative environmental research. A systematic review of the impact of virtual reality and natural environments on psychological well-being compares the effects of the two exposure modes [21]. The progress of virtual reality technology in mental health interventions summarizes its therapeutic potential [22], and empirical research shows that daily virtual nature exposure can effectively reduce anxiety symptoms [23]. The successful application of machine learning and big data technologies in urban spatial perception measurement provides methodological support for large-scale environmental assessment [24], but existing restorative environmental research mostly relies on subjective scales to obtain human perception data, and automated assessment methods based on objective environmental characteristics still need to be developed.

This study aims to design an AI-driven assessment framework for urban greenway restorative environments, addressing current deficiencies in the application of technology and the integration of theory. The specific objectives are to develop a deep learning-based feature extraction method for greenway street scenes; to construct a quantitative restorative assessment model based on attention restoration theory; and to verify the framework's effectiveness and interpretability. The novelty lies in three aspects: methodologically, proposing a complete "semantic segmentation – feature quantification – restorative mapping" process; theoretically, transforming the four dimensions of attention restoration theory into computable environmental indices; and practically, constructing an automatic evaluation tool for urban greenways. The research outcomes are expected to support greenway planning decisions and provide methodological reference for integrating AI with environmental psychology.

2. Methods

2.1 Research data

The greenway restoration environmental assessment framework developed in this research, using AI, relies on multi-source data such as street-view imagery, greenway vector networks, and semantic annotation datasets. During the acquisition and processing of the datasets, the Responsible Research for Urban Geospatial Artificial Intelligence guidelines [25] were followed. All images were obtained under the CC BY-SA 4.0 license, permitting academic use. Privacy protection was ensured through the Mapillary platform's automatic blurring of faces and license plates, and images containing identifiable individuals were excluded. To mitigate sampling bias, we maintained proportional representation across greenway types and restricted collection to consistent weather conditions.

The street views were obtained from the platform Mapillary (https://www.mapillary.com/), which provides open data and is governed by the CC BY-SA 4.0 license. This license allows academic use, as long as the platform is cited in the manuscript and the data statement. The empirical case study under investigation is the greenway system network in a city in the Yangtze River Delta, China. This area is the most urbanized in China and has advanced greenway infrastructure. The chosen city includes a variety of greenways within a small geographic area and comprehensive street views. Based on OpenStreetMap land-use attributes, greenways could be classified into three types within a 50-meter buffer zone: waterfront type (located near rivers and lakes), park type (located in and along green spaces), and street type (located along roads and buildings). These types of greenways matched the municipal greenway plans and could be verified using satellite images. These three types represent the dominant greenway categories in the Yangtze River Delta's dense water network and urban-rural mosaic landscape. The systematic differences among the three types of greenways in the composition of environmental elements offer excellent ground for future studies.

Image sampling was carried out by setting sampling points at 50-meter intervals along the greenway centerline [8, 15], and obtaining street-view images covering 120 degrees in the pedestrian movement direction at each point. After quality checks, the final valid sample consisted of 2,147 street-view images, classified into three greenway types: 728 waterfront images, 635 park images, and 784 street-type images. The images were all taken under sunny daytime conditions between 2022 and 2024, limited to the growing seasons (April to October), which ensured similar vegetation and lighting conditions. The sample size for each greenway category was relatively equal. Due to semantic imbalance, especially for water-body pixels, which accounted for only 5.5% of all pixels, a combined loss function was adopted as shown in Equation 3 to improve the model's ability to detect minority classes. Green space vector data extraction from the OpenStreetMap platform (https://www.openstreetmap.org/), based on the attribute

elements to build the greenway network data set and implement three kinds of green space classification notation.

The semantic segmentation model was trained using a pre-training-fine-tuning transfer learning paradigm, with the Cityscapes public dataset (https://www.cityscapes-dataset.com/) as the pre-training basis. This dataset contains 5000 finely pixel-labeled street view images. Covering 19 semantic categories. To address the environmental features of greenways, the study developed a fine-tuning dataset with 500 manually labeled images. We simplified the labeled categories into six types – vegetation, sky, water body, road, building, and others. Inter-annotator agreement reached Cohen's Kappa of 0.83. The dataset was split into training, validation, and test sets at a ratio of 70%, 10%, and 20%. The model's performance evaluation was done on a test set, which included Figure 1, depicting the technical route of the study, from data collection to recovery assessment.

2.2 Deep learning feature extraction

Previous studies have validated semantic segmentation for vegetation recognition [26] and demonstrated that multi-scale context modeling improves segmentation accuracy [27].

Given segmentation accuracy, computing efficiency and reproducibility, DeepLabV3+ was chosen as the main model. Transformer-based models like SegFormer have shown competitive performance recently, but they demand larger training datasets and more computational resources. With only 500 fine-tuning images available, DeepLabV3+ proved more suitable for balancing accuracy and training stability.

With the introduction of the dilation rate parameter r, the receptive field is expanded by dilated convolution without increasing parameters. The effective kernel size k_e is calculated as:

$$k_e = k + (k-1)(r-1) \quad (1)$$

where k denotes the original kernel size, and r is the dilation rate.

The ASPP module is configured in parallel with multiple convolutional branches of different expansion rates to achieve multi-scale feature fusion:

$$F_{ASPP} = Concat[F_1^{r_1}, F_2^{r_2}, F_3^{r_3}, F_{pool}] \quad (2)$$

where F^{r_i} denotes the output of the atrous convolution branch with a dilation rate r_i , and F_{pool} represents the output of the global average pooling branch.

This study adopts the classic configuration of $r_1 = 6$, $r_2 = 12$, and $r_3 = 18$ to systematically cover multi-level receptive field requirements ranging from local details to global scene context. The symmetrical structure design of the encoder-decoder gradually fuses the spatial detail information retained at each level of the encoder in the decoding upsampling stage, effectively alleviating the spatial resolution loss and boundary blurring problems caused by the continuous pooling downsampling operation, and significantly improving the segmentation sharpness and category determination accuracy of the object contour transition area.

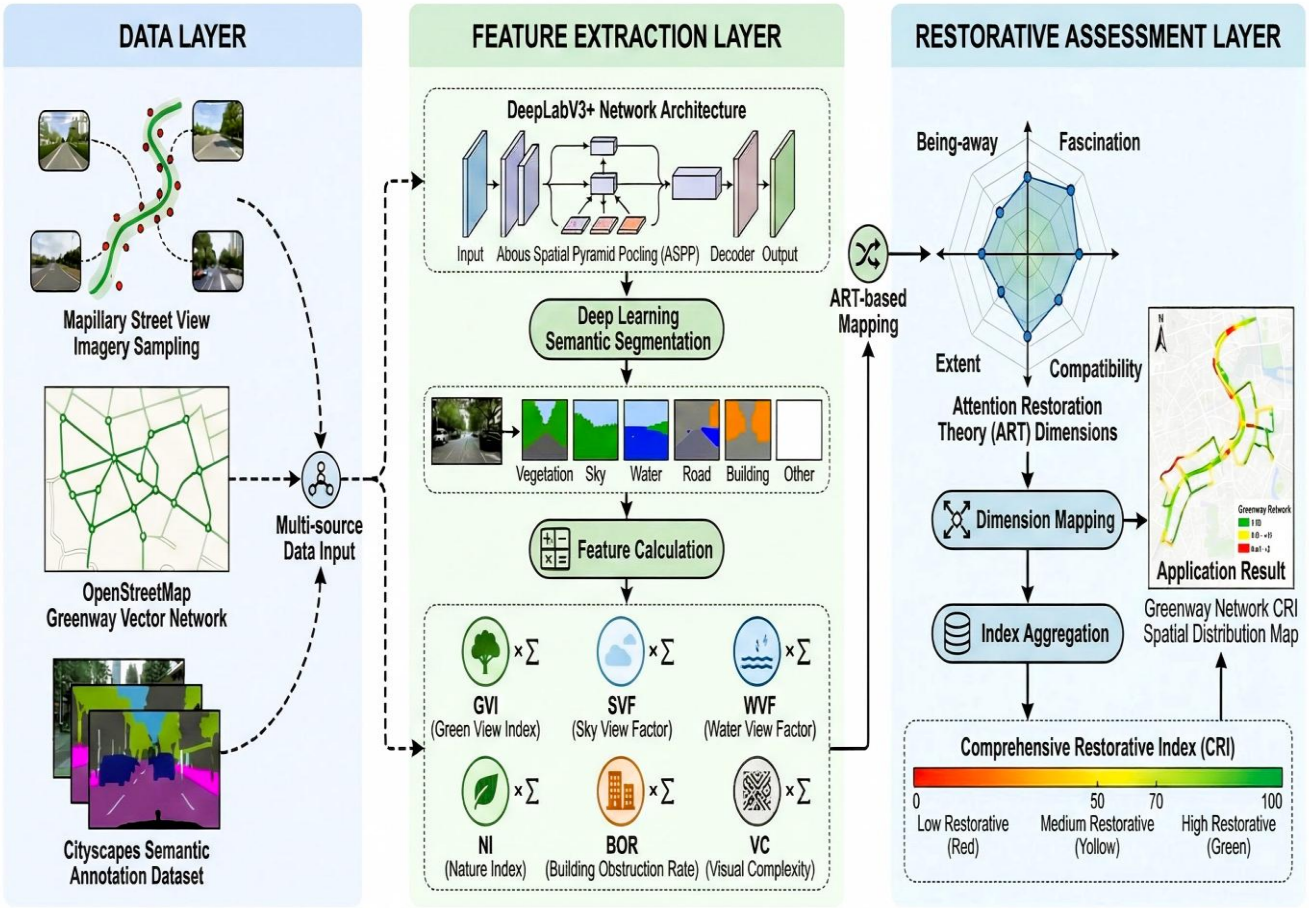

Figure 1. Technical framework of the AI-driven greenway restorative assessment

For the implementation of a ResNet-101 model, a network that is used for feature extraction in other computer vision frameworks. The 101-layer deep residual learning architecture of ResNet can effectively address the vanishing gradient problem during the training of deep networks through cross-layer quick connections and possesses a powerful ability to express hierarchical visual features. The step size of the network output is set to 8 to achieve a balance oriented towards engineering applications between inference computational efficiency and output spatial resolution. For model training, we use a stochastic gradient descent optimization algorithm, and for the loss function, we use a linear weighted combination of pixel-wise cross-entropy loss and Dice loss to mitigate class imbalance.

$$\mathcal{L} = \lambda_{CE}\mathcal{L}_{CE} + \lambda_{Dice}\mathcal{L}_{Dice} \quad (3)$$

$$\mathcal{L}_{CE} = -\frac{1}{N}\sum_{i}^{N}\sum_{C=1}^{C} y_{i,c}\, log(\hat{y}i, c) \quad (4)$$

$$\mathcal{L}_{Dice} = 1 - \frac{2\sum_i y_i \hat{y}_i}{\sum_i y_i + \sum_i \hat{y}_i} \quad (5)$$

$$lr = l_{r_0}(1 - \frac{iter}{max_{iter}})^{power} \quad (6)$$

where the cross-entropy loss $\mathcal{L}_{CE}$ quantifies pixel-level classification error, $\mathcal{L}_{Dice}$ optimizes region-level overlap, and λ_{CE} and λ_{Dice} are balancing coefficients, set to 0.5 and 0.5, respectively, in this study. The initial learning rate is set to 0.01 and decreases following a polynomial decay strategy with power = 0.9 to promote convergence stability. The initial learning rate is set to 0.01 and smoothly decreases during training following a polynomial decay scheduling strategy l_{r_0} to promote convergence stability. The momentum parameter is configured as 0.9 to accelerate directional consistency of parameter updates while suppressing gradient oscillations. The training batch size is set to 8, and the total number of training epochs is 100. Data augmentation strategies (random cropping, horizontal flipping, and color perturbation) enhance model generalization. This transfer learning paradigm has been validated in urban environment assessment research [28]. Based on the segmentation results, a quantitative index system for visual environment features is constructed. The index design follows two principles: depicting perceivable environmental features from the perspective of pedestrians and having an explainable conceptual connection with the restorative theory dimension. The theoretical correlation analysis between semantic categories and restorability is shown in Table 1.

Table 1 turns the attention recovery theory in its discussion of the restorative effect of nature into a set of determinacy rules for the semantic categories of street scenes: Vegetation, sky, and water bodies are the core categories of natural elements that may have restorative effects, while buildings and other artificial elements are possible restorative inhibitory factors. The influence of roads on restorative effects through greenways as a functional infrastructure is said to be neutral. Using this classification framework as the basis, we extract from the semantic segmentation outcomes six visual environment indicators: Green vision rate (GVI) measures the perceived concentration of vegetation; Sky visibility (SVF) indicates the openness of the space; Water visibility (WVF) measures the exposure of blue space; The naturalness index (NI) takes into account the proportion of nature; Building occlusion degree (BOR) indicates the interference of the artificial environment; Visual complexity (VC) measures the diversity of scenes, using Shannon entropy. The definition method for the above six indicators is consistent with existing studies on the street-view environment, ensuring the comparability and repeatability of the research results. The systematic description of each indicator is provided in Table 2. The six indicators listed in Table 2 characterize the visual feature structure of greenways across complementary perception dimensions, forming an intermediate representation layer from street-view images to restorative assessment models.

2.3 Recovery assessment framework

This study introduces attention recovery theory as a conceptual mediator, constructing a hierarchical mapping model of "visual features → theoretical dimensions → comprehensive index" to transform measurable environmental attributes into psychological perceptions. The empirical research on the link between environmental features and restorative perception provides a significant reference for the construction of the mapping model. Understanding the effects of different factors on the restorative perception of urban green Spaces sheds light on the significant differentiated effects of vegetation richness and spatial openness on the restorative dimension [29]. Objective greening indicators have been shown to predict subjective restorative experiences well [30]. Based on the evidence summarized above, the present study will operationalize the four dimensions of attention recovery theory – distance perception, attractiveness, extensibility, and compatibility – into computable indicators.

Table 1. Classification of environmental elements and their associations with restorative theory

Semantic Category	Element Type	Restorative Effect	Theoretical Rationale
Vegetation	Natural	Positive (+)	Possesses typical "soft fascination" characteristics, capable of effortlessly capturing attention without cognitive demand, serving as the core element for triggering restorative experiences
Sky	Natural	Positive (+)	Provides vertical spatial openness, enhances the "extent" dimension experience, and facilitates psychological escape from everyday environments
Water	Natural	Positive (+)	Dynamic light reflections and rhythmic movements on water surfaces offer unique visual attraction, contributing significantly to the "fascination" dimension
Road	Artificial	Neutral (○)	Functions as greenway infrastructure supporting walking and cycling activities, providing supportive effects on the "compatibility" dimension
Building	Artificial	Negative (−)	Obstructs natural views and increases perception of artificial interference, weakening the "being-away" dimension and reducing overall restorative potential
Other	Artificial	Negative (−)	Encompasses heterogeneous elements such as vehicles, facilities, and pedestrians, increasing scene complexity and urbanization perception with mild negative effects on restorativeness

Table 2. Visual environmental feature indicators: definitions and calculation methods

Indicator	Full Name	Definition	Theoretical Association
GVI	Green View Index	Proportion of vegetation pixels in the total image area, reflecting the visual dominance of greenery from a pedestrian perspective	Primary contributor to "fascination" dimension; higher values generally associated with stronger restorative potential
SVF	Sky View Factor	Proportion of sky pixels in the total image area, quantifying vertical spatial openness	Primarily associated with "extent" dimension; contributes to perception of spaciousness and psychological relief
WVF	Water View Factor	Proportion of water pixels in the total image area, measuring visual exposure to blue space elements	Contributes to "fascination" dimension; particularly relevant for waterfront greenways
NI	Nature Index	Cumulative proportion of natural elements (vegetation, sky, water) in the image	Composite indicator for "being-away" dimension; reflects overall naturalness of the scene
BOR	Building Obstruction Ratio	Proportion of building pixels in the total image area, indicating artificial encroachment on visual field	Negative contributor to "being-away" dimension; higher values tend to reduce restorative potential
VC	Visual Complexity	Shannon entropy-based measure of semantic category distribution diversity and evenness	Moderate complexity may support "fascination" through visual interest; excessive complexity potentially causes cognitive overload

Table 3. Operationalization framework of attention restoration theory dimensions

Dimension	Abbreviation	Conceptual Definition	Related Indicators	Operationalization Rationale
Being-away	BA	The capacity of an environment to facilitate psychological detachment from everyday work contexts and provide a sense of "being elsewhere"	NI (+), BOR (−)	High naturalness and low building obstruction support escape experiences [29, 33]; weights determined via AHP with $\alpha_1 + \alpha_2 = 1$
Fascina -tion	FA	The richness of elements that can spontaneously attract attention without requiring cognitive effort, characterized by "soft fascination"	GVI (+), WVF (+), VC (+)	Vegetation, water, and moderate visual complexity provide effortless attention capture [17, 37]; weights $\sum_{i=1}^{3} \beta_i = 1$
Extent	EX	The characteristics of environmental space in terms of scope and coherence, supporting immersive "another world" experiences	SVF (+), CON (+)	Sky openness and landscape continuity contribute to spatial expansiveness [20, 30]; continuity calculated via cosine similarity with $\gamma_1 + \gamma_2 = 1$
Compatibility	CO	The degree to which the environment supports current activity purposes and behavioral inclinations	Road ratio	Road proportion serves as proxy for walkability and cycling suitability [3, 4]; limited by single-image constraints

The sense of distance (BA) involves the environment's ability to enable the individual to have a psychological experience of escape, characterised by the feeling of being elsewhere, and is associated with the degree of naturalness and the level of artificial interference present. Charm (FA) captures the wealth of soft-charm elements in the environment that may spontaneously catch attention without cognitive effort. The extent and coherence of the environmental space is labeled extensibility, such as linear spaces, in the case of greenways. Matching the environment in which activities occur with the required laid-back and sporty character. Table 3 describes the 4D operationalization framework. Table 3 illustrates the transformation from abstract ART concepts to computable indicators. Dimension scores are computed as weighted linear combinations of relevant visual feature indicators, following the multi-attribute utility theory framework in environmental perception. The weight coefficients were obtained using the Analytic Hierarchy Process (AHP). Five environmental psychologists and urban planners were asked to construct pairwise comparison matrices based on importance rankings. The geometric mean method was used to compute the

aggregated judgment matrix, and the eigenvector method was used to obtain the final weights. The aggregated judgment matrix is shown in Table 4.

Table 4. Aggregated AHP judgment matrix for CRI dimension weights

	BA	FA	EX	CO
BA	1	1/2	1	2
FA	2	1	2	3
EX	1	1/2	1	2
CO	1/2	1/3	1/2	1

Note: Principal eigenvalue λmax = 4.02, Consistency Index CI = 0.007, Consistency Ratio CR = 0.008 < 0.1.

The aggregated pairwise comparison matrix is shown in Table 4 and was developed based on input from five experts across the four dimensions of ART. The values above the diagonal represent the ratios of importance; for instance, FA is twice as important as BA in restorative assessment. This matrix met the consistency criteria (λmax = 4.02, CI = 0.007, CR = 0.008 < 0.1).

The four-dimensional scores are then integrated through weighted aggregation to generate a comprehensive recovery index (CRI), which reflects the overall restorative potential of the greenway environment:

$$CRI = \omega_1 \cdot BA + \omega_2 \cdot FA + \omega_3 \cdot EX + \omega_4 \cdot CO, \sum_{i=1}^{4} \omega_1 = 1 \quad (7)$$

Based on the ranking of functional importance across dimensions according to Attention Restoration Theory, fascination, as the core triggering mechanism of restorative experience, is assigned the highest weight. The final weights are determined as$\omega_1 = 0.25$, $\omega_2 = 0.35$, $\omega_3 = 0.25$, and $\omega_4 = 0.15$, with the consistency ratio $CR < 0.1$ satisfying the consistency requirement of the judgment matrix. The CRI scale ranges from 0 to 100, and there are three levels of greenway restorativeness based on CRI: CRI ≥ 70, indicating high restorative environments; 50 ≤ CRI < 70, indicating moderate restorative environments; and CRI < 50, indicating low restorative environments. These classes were determined using the natural breaks (Jenks) classification method of the CRI distribution of all samples.

3. Results

3.1 Verification of feature extraction models

The precision of feature extraction is directly influenced by the efficiency of semantic segmentation models. Errors in critical restorative components, such as trees, shrubs, vegetated ground covers, and water bodies, will result in systematic errors in visual environment indicators calculated afterward. To ensure technical reliability, it is therefore necessary to perform system performance verification on the selected model. This study conducted a comparative experiment between DeepLabV3+ and several mainstream baseline models on the greenway street-view test set (322 images, 15% of the total sample). The metrics used to evaluate performance included pixel accuracy (PA), mean intersection and union ratio (mIoU), and Macro-F1 score. The mIoU metric is the most important measure. It takes into account the per-category segmentation performance and the category balance. Further, it considers the overall segmentation quality. The comparison baselines included FCN-8s, U-Net, and PSPNet. In the interest of fairness, the same training configuration (initial learning rate 0.01, 100 epochs, and the same data augmentation strategy) was used by all models. The results are shown in Table 5.

Table 5. Performance comparison of different semantic segmentation models

Model	Backbone	PA (%)	mIoU (%)	Macro-F1 (%)	Inference Time (ms/image)
FCN-8s	VGG-16	81.4	67.6	78.2	44
U-Net	ResNet-50	85.2	71.8	84.3	53
PSPNet	ResNet-101	85.9	75.1	84.5	66
DeepLabV3+	ResNet-101	89.6	78.3	87.6	71

Table 5 results indicate that DeepLabV3+ achieves the best performance among all three indicators (mIoU=78.3%, PA=89.6%). Meanwhile, the void space pyramid pooling the module captures semantic features of multi-scale environment elements in the greenway scene well enough to lay a reliable technical foundation for subsequent restorability assessment.

The assessment of restoration can significantly vary with the segmentation accuracy of categories. The essential condition of greenery and water, which promotes restorative effects, according to the Attention Restoration Theory (ART), the recognition rate directly affects green vision rate (GVI), water visibility (WVF), and other key indicators, and credibility calculation of greens in the urban environment. This is subsequently communicated to the assessment results of the four-dimensional recovery score and the comprehensive recovery Index (CRI). Identifying the accuracy of building categories is equally vital, as building occlusion (BOR) serves a negative, restorative inhibitory role within the assessment framework. It is thus required to carry out a finer analysis of the segmentation performance of deepLabV3+ across different semantic categories, as well as to evaluate its capability to recognize essential elements embedded in restorative assessment. The title indicates that it refers to segmented accuracy for each category. Table 6 shows the segmented accuracy of each category.

According to the results shown in Table 6, the vegetation category reached high segmentation accuracy (IoU=84.2%), providing reliable input for green view rate calculation. The water body class showed a relatively low IoU (72.5%), mainly due to a limited sample proportion (5.5%) and visual variability caused by surface reflections. Notably, precision (86.2%) exceeded recall (81.7%) for water, suggesting conservative predictions that missed some water pixels. To illustrate the model's segmentation effect in different greenway types and verify its adaptability to complicated environments, one typical case of the three types of greenway test samples is selected for visual comparative analysis. The choice of cases considers both representativeness and challenge: the waterfront case features an intricate junction among water, greening, and shorelines; the park-type case features scenes of large-scale, continuous greening coverage; and the street-type case features a highly mixed composite environment of buildings, greening, and roads. In each case, the original street-view images, manually labeled Ground Truth labels, and model prediction results are shown side by side.

Table 6. Semantic segmentation accuracy of DeepLabV3+ by category

Category	IoU (%)	Precision (%)	Recall (%)	F1 (%)	Sample Proportion (%)	Accuracy Characteristics
Vegetation	84.2	91.3	89.9	90.6	36.1	Dominant category with stable performance; minor confusion at vegetation-building boundaries
Sky	88.3	94.1	92.8	93.5	21.4	Highest accuracy due to distinctive color features and clear boundaries
Water	72.5	86.2	81.7	83.9	5.5	Lower accuracy due to limited samples and variable surface reflections
Road	81.1	88.5	90.2	89.3	18.6	Stable performance; occasional misclassification with similar-textured surfaces
Building	76.4	84.8	87.6	86.2	13.5	Moderate accuracy; shadows and partial occlusions affect boundary precision
Other	66.1	77.3	81.6	79.4	4.9	Lowest accuracy due to high intra-class heterogeneity of miscellaneous elements

To establish an intuitive correspondence between segmentation quality and evaluation results, the CRI value for the sampling point is also labeled at the same time. The visualization results are shown in Figure 2. Figure 2 shows that the model can well identify the main environmental elements in all three types of scenarios. The boundaries between vegetation and the sky are clear. In the waterfront case, the water body is effectively identified. Although there are sporadic misclassifications in the street-type case, the overall requirements for feature quantification are met.

3.2 Greenway restorative assessment results

Once the semantic segmentation model has been verified, this study will apply it to all 2,147 greenway street-view sampling points. Using batch reasoning, dataset-level pixel-level annotations were obtained for six indicators: visual environmental feature GVI, SVF, WVF, NI, BOR, and VC. From this, the 4D scores (BA, FA, EX, CO) and the comprehensive recovery index (CRI) of attention recovery theory can be calculated. Due to the systematic differences in location conditions and landscape configuration, the three types of greenways are anticipated to show significant inter-group differences in environmental characteristics and recovery scores: waterfront greenways have an advantage in the expected water-related indicators, park type has the highest expected green view rate, and street type greenways show a higher expected building shading degree and lower recovery score due to the interference of the built environment. To verify the above expectations and disclose the influence mechanism of the group recoverability combination of different environmental features, descriptive statistics of the indicators for the three types of greenways were prepared, and then the differences among the groups were analyzed using One-way ANOVA. The results are shown in Table 7.

Table 7 results aligned with theoretical expectations: park-type greenways had the highest GVI (45.6%), waterfront type the highest WVF (12.3%), and street type the highest BOR (32.6%) with the lowest CRI (50.1). Waterfront CRI (68.2) slightly exceeded park type (66.5) due to water body contributions to the fascination dimension.

ANOVA confirmed significant between-group differences for GVI, WVF, and BOR ($p<0.001$), SVF ($p<0.01$), and VC ($p<0.05$). Comparing the four-dimensional restorative scores across greenway types reveals how environmental features translate into psychological perception.

The different score profiles of various types of greenways in the four dimensions of distance perception, BA, attractiveness, FA, extensibility, EX, and compatibility, CO, can directly reflect their restorative advantages and disadvantages. Waterfront greenway paths are expected to be more pleasant than non-waterfront paths because the water body element offers a dynamic aesthetic. Due to high naturalness and low artificial interference, the park greenway paths are expected to be prominent in the distance dimension. Conversely, it is anticipated that street greenway paths will receive lower scores across nearly all components due to architectural obstructions or a lack of natural features. To make the differences in the recovery contours of the three types of greenway tracks more intuitive, Figure 3 shows a radar chart comparing scores across four dimensions. The contour area of the radar chart directly reflects the overall recovery potential.

Figure 3 clearly shows that the radar contours for the waterfront and park-type greenways are significantly larger than those for the street-type greenways. The waterfront type has the highest charm score (FA=72.6), which is attributed to the visual appeal of the water body, while the park type has the highest distance perception score (BA=72.1), which is due to the natural escape experience created by the rich vegetation. The spatial distribution characteristics of the Comprehensive Recovery Index (CRI) have direct application value for urban greenway planning. By identifying the spatial positions of the recovery "hotspots "(high CRI sections) and" cold spots "(low CRI sections) in the greenway system, the planning management department can formulate targeted environmental improvement strategies. In this study, the CRI results for all sampling points were correlated with the spatial vector data for the binding channels.

Table 7. Visual environmental features and restorative scores by greenway type

Indicator		Waterfront (n=728)	Park (n=635)	Street (n=784)	F	p
Visual Environmental Features	GVI (%)	38.2±12.4	45.6±10.8	25.3±14.2	91.4	<0.001
	SVF (%)	24.5±8.7	22.1±7.3	18.9±9.8	12.8	<0.01
	WVF (%)	12.3±8.9	3.5±4.2	0.8±2.1	136.8	<0.001
	NI (%)	73.8±11.2	70.9±9.5	44.7±15.6	89.6	<0.001
	BOR (%)	9.2±7.8	10.4±8.5	32.6±15.3	109.5	<0.001
	VC (bits)	2.12±0.36	2.05±0.32	2.19±0.41	3.7	<0.05
ART Dimension Scores	BA	70.5±10.2	72.1±8.9	48.5±13.6	86.3	<0.001
	FA	72.6±11.8	79.4±9.4	45.2±14.1	88.7	<0.001
	EX	65.8±12.3	64.2±10.7	52.4±11.8	35.7	<0.001
	CO	62.3±9.5	60.5±8.8	58.7±10.4	4.2	<0.05
Comprehensive Index	CRI	68.2±11.3	66.5±9.6	50.1±14.8	76.8	<0.001

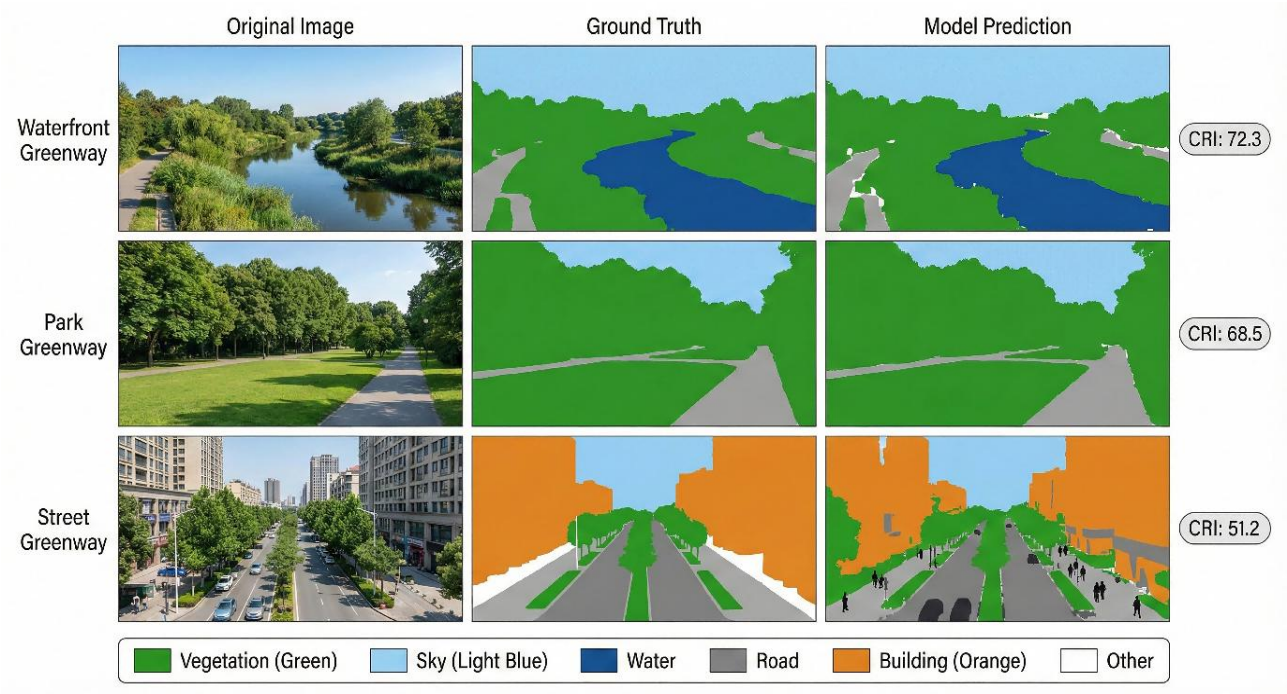

Figure 2. Visualization of semantic segmentation results for three types of greenway street scenes

According to the classification criteria defined in the method section (high recovery, medium recovery, and low recovery), each sampling point was assigned to a grade, and the spatial distribution of CRI along the binding channel network was presented as a heat map. To reveal the spatial heterogeneity characteristics of restorative environmental quality, the results are shown in Figure 4.

Figure 4 shows that the high-recovery sections (23.5%) are concentrated in waterfront landscape nodes and park core areas, while the low-recovery sections (22.3%) are mainly distributed along street-type bound roads near major traffic arteries and commercial areas.

The medium-recovery sections are the most widely distributed (accounting for 54.2%).

3.3 Verification of the validity of the evaluation framework

The credibility of restorative assessment results depends on a good assessment framework and systematic verification from two fronts: theoretical consistency and methodological robustness. Theoretical consistency verification assesses whether the recovery index derived from visual characteristics is consistent with the basic hypothesis of the attention recovery theory. The attention recovery theory

clearly holds that natural elements (vegetation in particular) possess a "soft charm" that can easily attract unintentional attention, thereby promoting the recovery of directed attention. An environment with natural elements should have a greater recovery potential. But artificially created elements can have an inhibiting effect. When the calculated CRI of this study aligns with the theoretically predicted directions (i.e., positive with GVI and NI, and negative with BOR), the evaluation framework is considered theoretically valid. In this way, the directional and intensity features of their association with recovery can be quantitatively evaluated by using the Pearson correlation coefficients between each visual environment feature index and CRI. Scatter plots and regression lines are used to visually show the linear relationship patterns between variables. The results of the correlation analysis are shown in Figure 5.

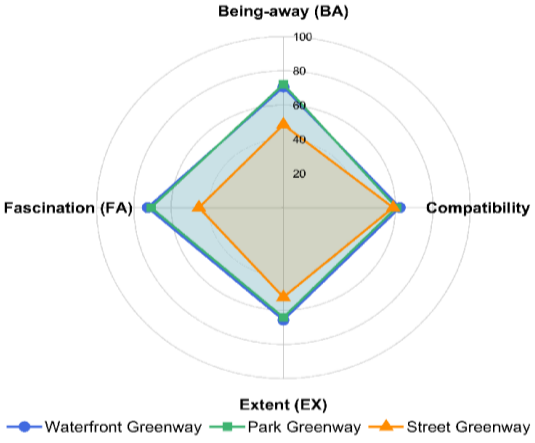

Figure 3. Comparison of the four-dimensional scores of the three types of greenway attention restoration theory

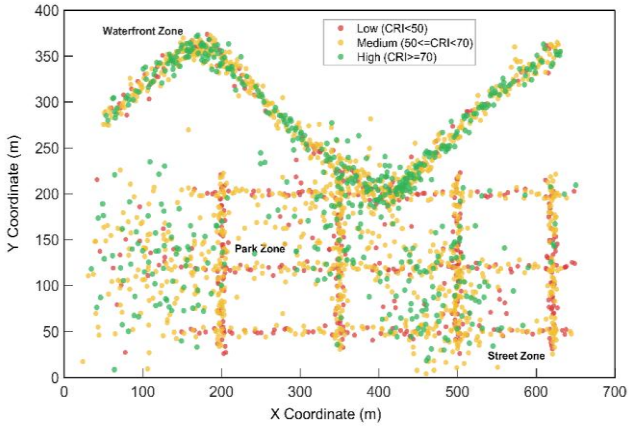

Figure 4. Spatial distribution of the comprehensive recovery index (CRI) of the greenway network

Figure 5 presents the correlation analysis between six visual environmental features and the Comprehensive Restorative Index (CRI). Among all indicators, GVI demonstrates the strongest positive correlation with CRI ($r=0.74$, $p<0.001$), confirming vegetation coverage as the primary contributor to restorative potential in greenway environments. NI exhibits a similarly strong positive association ($r=0.71$, $p<0.001$), reflecting the composite effect of natural elements on psychological restoration. In contrast, BOR shows a significant negative correlation ($r=-0.61$, $p<0.001$), supporting the theoretical prediction that building obstruction inhibits restorative experiences by disrupting the "being-away" dimension. WVF displays a moderate positive relationship ($r=0.56$, $p<0.001$), indicating that water visibility contributes meaningfully to the "fascination" dimension, particularly in waterfront greenways. SVF presents a weaker positive correlation ($r=0.43$, $p<0.01$), suggesting that sky openness plays a secondary role in restorative assessment. VC exhibits the weakest association ($r=0.28$, $p<0.01$), implying that visual complexity has a limited influence on overall restorative potential. The correlation patterns align consistently with predictions from Attention Restoration Theory, providing empirical support for the theoretical validity of the proposed assessment framework. Correlation should not be confused with causation. While these observations do match the ART model, they do not allow us to conclude that changes in visual features cause changes in restorative perception.

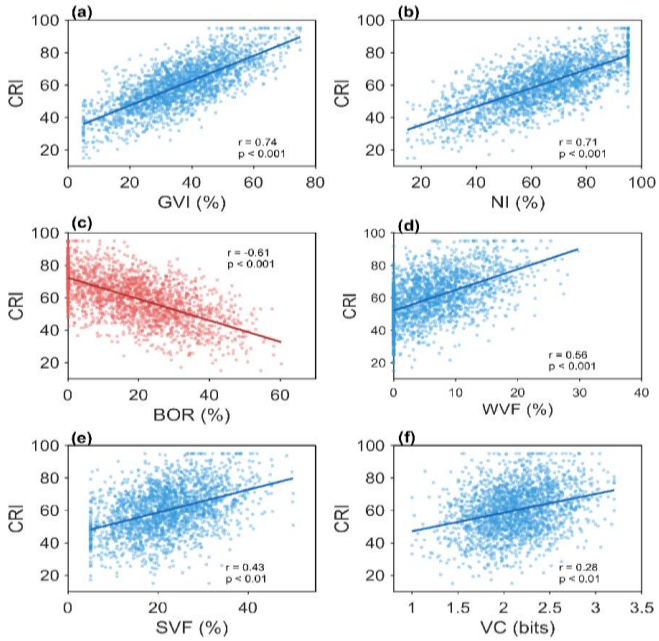

Figure 5. Correlation analysis between visual environment features and comprehensive recovery index (a) GVI vs CRI; (b) NI vs CRI; (c) BOR vs CRI; (d) WVF vs CRI; (e) SVF vs CRI; (f) VC vs CRI. Blue indicates positive correlations; red indicates negative correlations.

The overall association pattern between features and recoverability can be obtained using correlation analysis, but it cannot quantify the contribution degree of features to evaluation results and their influence mechanism. In order to fully understand the "black box" process of restorative assessment and interpretability of the framework, we use in this study SHAP(SHapley Additive exPlanations) which helps in feature importance analysis. SHAP applies the cooperative game theory's Shapley value concept to explain individual inputs. This method assesses how each characteristic affects the forecast outcome by computing the mean marginal contribution of each to all possible combinations of specified features. Compared with traditional feature importance indicators, SHAP can not only provide an importance ranking but also reveal the relationship between the level of eigenvalues and the direction of contribution (that is, whether a high eigenvalue has a positive or negative impact). A

Random Forest regression model was built using six indicators for the visual environment and CRI as the outcome variable. SHAP values were then calculated from the regression model. The Random Forest method was chosen because it is compatible with SHAP's TreeExplainer and has the ability to handle non-linear relationships between variables. This generated a SHAP summary graph, which shows the importance of each feature and its influence pattern. The results are shown in Figure 6.

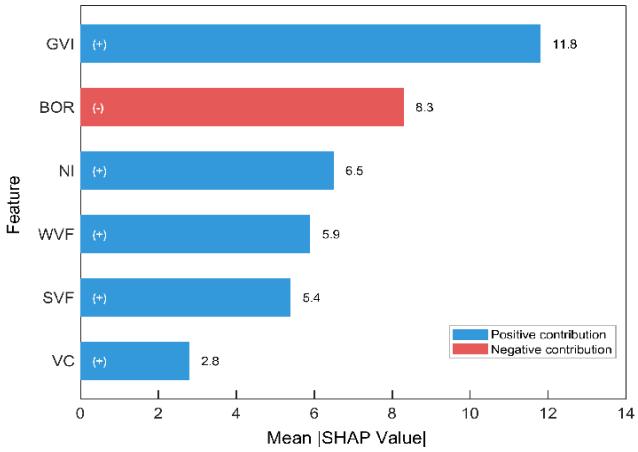

Figure 6. Analysis of the importance of recovery influencing factors based on SHAP

Figure 6 shows SHAP-based feature importance. GVI contributes most positively to CRI, whereas BOR contributes negatively. NI, WVF, SVF, and VC follow in descending order of importance. The robustness of the evaluation framework is an important guarantee of its practical application value. If the CRI calculation is highly sensitive to minor variations in dimension weights, the framework's reliability will be questioned. This study examines the dependence of evaluation results on parameter settings through the weight sensitivity analysis, comparing four weight configuration schemes: the original scheme is determined by the Analytic Hierarchy Process ($\omega_1 = 0.25$, $\omega_2 = 0.35$, $\omega_3 = 0.25$, $\omega_4 = 0.15$); the equal-weight scheme assumes all four dimensions are equally important (each being 0.25); the fascination-enhanced scheme increases by 10 percentage points to 0.45; and the being-away-enhanced scheme increases to 0.35. For each scheme, the CRI values of all sampling points are calculated and subjected to Spearman rank correlation analysis with the original scheme.

If the Spearman correlation coefficient approaches 1, it indicates that the relative ranking of sampling points remains stable across different schemes, meaning the evaluation conclusions are not substantially affected by minor weight adjustments. The sensitivity analysis results are shown in Table 8.

Table 8 shows that the mean CRI varied slightly (60.3–62.8) across the five weighting schemes. Spearman correlations between the original and alternative schemes ranged from 0.87 to 0.94, with the FA-enhanced scheme showing the highest correlation (0.94) and the equal-weight scheme the lowest (0.87). Although weight allocation affects absolute scores, the ranking pattern remains stable, confirming the framework's robustness.

4. Discussion

This research constructed an AI-driven environmental assessment framework for greenway restoration. It has shown good technical efficiency and theoretical validity through empirical tests. The DeepLabV3+ model's average intersection-over-union ratio of 78.3% and pixel accuracy of 89.6% demonstrate that deep learning can automatically identify multi-scale environmental elements in a greenway setting. The research study on the detection of street green space types based on machine learning, as referenced, provides methodological evidence [31]. The ratio of intersection to union across vegetation categories is 84.2%, providing a reliable reference for calculating the green view rate. Nonetheless, the water body category, with a comparatively low accuracy of 72.5%, highlights the universal shortcomings of small-sample categories in deep learning training. Research by Huang multiple cites the effects of representativeness of training samples on recognition of rare categories. For example, 34% of training samples for high-end clothing products fail the test sample classification, as cited in this research paper [32].

According to attention recovery theory, the "soft charm" property of vegetation fosters recovery experience. The green vision rate is strongly positively correlated with the recovery index, confirming this main proposition. There is also research on the relationship between exposure to green space and psychological stress perception, showing that vegetation coverage is associated with certain mental health indicators [33]. A strong negative relationship between "occupancy" of the environment and the ability to restore proved to inhibit the creation of built environment elements on recovery. The examination of the influence of street and canyon visuals on human perception shows that the degree of enclosure of buildings negatively affects the evaluation of environmental comfort [34].

Table 8. Sensitivity and robustness test of CRI weight schemes

Weight Scheme	BA	FA	EX	CO	CRI Mean	CRI SD	Spearman rho	Ranking Consistency
Original (AHP-based)	0.25	0.35	0.25	0.15	61.7	12.9	1.000	Reference
Equal weight	0.25	0.25	0.25	0.25	60.3	11.8	0.87	High
FA-enhanced	0.20	0.45	0.20	0.15	62.8	13.1	0.94	Very High
BA-enhanced	0.35	0.30	0.20	0.15	62.1	12.4	0.91	Very High
EX-enhanced	0.20	0.30	0.35	0.15	61.2	12.6	0.89	High

The SHAP analysis revealed that green view rate is the primary restorative contribution factor, consistent with the conclusion in the Shanghai Street View Perception Study that greening elements have an important impact on environmental quality evaluation [35]. The structural equation model analysis of environmental characteristics and perceived restorability of rooftop gardens also confirmed that vegetation richness is a key predictor of restorability [36]. The differences observed in the four-dimensional restorative scores can help explain the assessment framework's sensitivity across heterogeneous settings across the three types of greenways. The study showed that dynamic aspects of water bodies can increase the restorative potential of nature [37].

The framework has been validated in one city and has yet to be tested across cities with different climates, densities, and cultural settings. The integration of objective and subjective measures may provide a more comprehensive view [38]. The proposed assessment has not yet integrated dynamic aspects of the environment, but has used static street-view images. Future development may integrate Virtual Reality/AR technology to provide simulations of greenways in a virtual environment [39], enabling controlled experiments to compare exposure in the actual and virtual environments [40]. The paradigm of "data-driven feature extraction and theory-guided evaluation" presented in this study provides an exploratory approach to integrate artificial intelligence with Environmental Psychology.

5. Conclusions

The present study develops an assessment framework for the restorative environment of urban greenways using deep-learning semantic segmentation technology, street-view image data, and attention recovery theory. This process of "visual feature extraction-theoretical dimension mapping-comprehensive index calculation" realizes the objective and automatic evaluation of the greenways' rehabilitation potential. The empirical results show that the DeepLabV3+ model performs well on the greenway scene segmentation task, achieving a cross-union ratio of 78.3%. The four-dimensional recovery scores across the three types of greenways differ significantly. The impact of green vision degree and building occlusion degree on the recovery index is positive and negative, respectively. The study results can act as a scientific evaluation tool for evidence-based urban greenway planning and design. They also offer a methodological reference for the interdisciplinary combination of artificial intelligence technology and environmental psychology theory.

Ethical issue

The authors are aware of and comply with best practices in publication ethics, specifically regarding authorship (avoidance of guest authorship), dual submission, manipulation of figures, competing interests, and compliance with research ethics policies. The authors adhere to publication requirements that the submitted work is original and has not been published elsewhere.

Data availability statement

The manuscript contains all the data. However, more data will be available upon request from the authors.

Conflict of interest

The authors declare no potential conflict of interest.

References

[1] Li Z., et al., Large-scale greenway exposure reduces sedentary behavior: a natural experiment in China. Health & Place, 2024. 89: p. 103283. https://doi.org/10.1016/j.healthplace.2024.103283.

[2] Deng Y., J. Liang, and Q. Chen, Greenway interventions effectively enhance physical activity levels—A systematic review with meta-analysis. Frontiers in Public Health, 2023. 11: p. 1268502. https://doi.org/10.3389/fpubh.2023.1268502.

[3] Vatanparast E., et al., Urban greenway planning: Identifying optimal locations for active travel corridors through individual mobility assessment. Urban Forestry & Urban Greening, 2024. 101: p. 128464. https://doi.org/10.1016/j.ufug.2024.128464.

[4] Fu E., et al., Exploring Restrictions to use of community greenways for physical activity through structural equation modeling. Frontiers in Public Health, 2023. 11: p. 1169728. https://doi.org/10.3389/fpubh.2023.1169728.

[5] Naghibi M., A. Farrokhi, and M. Faizi, Small urban green spaces: insights into perception, preference, and psychological well-being in a densely populated areas of Tehran, Iran. Environmental Health Insights, 2024. 18: p. 11786302241248314. https://doi.org/10.1177/11786302241248314.

[6] Liu L., et al., Restorative benefits of urban green space: Physiological, psychological restoration and eye movement analysis. Journal of environmental management, 2022. 301: p. 113930. https://doi.org/10.1016/j.jenvman.2021.113930.

[7] Hung S.-H., Does perceived biophilic design contribute to human well-being in urban green spaces? A study of perceived naturalness, biodiversity, perceived restorativeness, and subjective vitality. Urban Forestry & Urban Greening, 2025. 107: p. 128752. https://doi.org/10.1016/j.ufug.2025.128752.

[8] Zhou Y., et al., Measuring and understanding changes in the physical built environment of cities with street view images. Urban Informatics, 2025. 4(1): p. 3. https://doi.org/10.1007/s44212-025-00069-9.

[9] Lee D.H., H.Y. Park, and J. Lee, A review on recent deep learning-based semantic segmentation for urban greenness measurement. Sensors, 2024. 24(7): p. 2245. https://doi.org/10.3390/s24072245.

[10] Zhang L., et al., Decoding urban green spaces: Deep learning and google street view measure greening structures. Urban Forestry & Urban Greening, 2023. 87: p. 128028. https://doi.org/10.1016/j.ufug.2023.128028.

[11] Kameoka T., et al., Assessing streetscape greenery with deep neural network using Google Street View. Breeding Science, 2022. 72(1): p. 107-114. https://doi.org/10.1270/jsbbs.21073.

[12] Ma Y., et al., From Sky to Ground: Monitoring Visible Street Greenery via Multisource Remote Sensing Imagery with Deep Learning. Urban Forestry & Urban Greening, 2025: p. 128866. https://doi.org/10.1016/j.ufug.2025.128866.

[13] Perez J. and G. Fusco, Streetscape Analysis with Generative AI (SAGAI): Vision-language assessment

and mapping of urban scenes. Geomatica, 2025: p. 100063. https://doi.org/10.1016/j.geomat.2025.100063.
[14] Hu A., N. Yabuki, and T. Fukuda, Multi-temporal analysis of urban vegetation using deep learning and 3D reconstruction. Landscape Ecology, 2025. 40(7): p. 125. https://doi.org/10.1007/s10980-025-02090-4.
[15] Ma X., et al., Measuring human perceptions of streetscapes to better inform urban renewal: A perspective of scene semantic parsing. Cities, 2021. 110: p. 103086. https://doi.org/10.1016/j.cities.2020.103086.
[16] Qi Y., et al., An investigation of the visual features of urban street vitality using a convolutional neural network. Geo-spatial Information Science, 2020. 23(4): p. 341-351. https://doi.org/10.1080/10095020.2020.1847002.
[17] Liu Y., et al., A review of attention restoration theory: Implications for designing restorative environments. Sustainability, 2024. 16(9): p. 3639. https://doi.org/10.3390/su16093639.
[18] Menardo E., et al., Restorativeness in natural and urban environments: A meta-analysis. Psychological Reports, 2021. 124(2): p. 417-437. https://doi.org/10.1177/003329411988406.
[19] Bornioli A. and M. Subiza-Pérez, Restorative urban environments for healthy cities: A theoretical model for the study of restorative experiences in urban built settings. Landscape Research, 2023. 48(1): p. 152-163. https://doi.org/10.1080/01426397.2022.2124962.
[20] Huang S., et al., The contribution to stress recovery and attention restoration potential of exposure to urban green spaces in low-density residential areas. International journal of environmental research and public health, 2021. 18(16): p. 8713. https://doi.org/10.3390/ijerph18168713.
[21] Liang L., et al., Urban Green Spaces and Mental Well-Being: A Systematic Review of Studies Comparing Virtual Reality versus Real Nature. Future Internet, 2024. 16(6): p. 182. https://doi.org/10.3390/fi16060182.
[22] Bell I.H., et al., Advances in the use of virtual reality to treat mental health conditions. Nature Reviews Psychology, 2024. 3(8): p. 552-567. https://doi.org/10.1038/s44159-024-00334-9.
[23] Browning M.H., et al., Daily exposure to virtual nature reduces symptoms of anxiety in college students. Scientific reports, 2023. 13(1): p. 1239. https://doi.org/10.1038/s41598-023-28070-9.
[24] Ramírez T., et al., Measuring heterogeneous perception of urban space with massive data and machine learning: An application to safety. Landscape and Urban Planning, 2021. 208: p. 104002. https://doi.org/10.1016/j.landurbplan.2020.104002.
[25] Marasinghe R., et al., Towards responsible urban geospatial AI: insights from the white and grey literatures. Journal of Geovisualization and Spatial Analysis, 2024. 8(2): p. 24. https://doi.org/10.1007/s41651-024-00184-2.
[26] Wang J., W. Liu, and A. Gou, Numerical characteristics and spatial distribution of panoramic Street Green View index based on SegNet semantic segmentation in Savannah. Urban Forestry & Urban Greening, 2022. 69: p. 127488. https://doi.org/10.1016/j.ufug.2022.127488.
[27] Shao Y., A.J. Cooner, and S.J. Walsh, Assessing deep convolutional neural networks and assisted machine perception for urban mapping. Remote Sensing, 2021. 13(8): p. 1523. https://doi.org/10.3390/rs13081523.
[28] Huang X., et al., Comprehensive walkability assessment of urban pedestrian environments using big data and deep learning techniques. Scientific Reports, 2024. 14(1): p. 26993. https://doi.org/10.1038/s41598-024-78041-x.
[29] Wang S. and A. Li, Identify the significant landscape characteristics for the perceived restorativeness of 8 perceived sensory dimensions in urban green space. Heliyon, 2024. 10(7) : e27925. https://doi.org/10.1016/j.heliyon.2024.e27925.
[30] Spano G., et al., Objective greenness, connectedness to nature and sunlight levels towards perceived restorativeness in urban nature. Scientific Reports, 2023. 13(1): p. 18192. https://doi.org/10.1038/s41598-023-45604-3.
[31] Sun Y., et al., Using machine learning to examine street green space types at a high spatial resolution: Application in Los Angeles County on socioeconomic disparities in exposure. Science of The Total Environment, 2021. 787: p. 147653. https://doi.org/10.1016/j.scitotenv.2021.147653.
[32] Wang R., et al., The distribution of greenspace quantity and quality and their association with neighbourhood socioeconomic conditions in Guangzhou, China: A new approach using deep learning method and street view images. Sustainable Cities and Society, 2021. 66: p. 102664. https://doi.org/10.1016/j.scs.2020.102664.
[33] Zhang T., et al., Assessing the nonlinear impact of green space exposure on psychological stress perception using machine learning and street view images. Frontiers in Public Health, 2024. 12: p. 1402536. https://doi.org/10.3389/fpubh.2024.1402536.
[34] Xu J., et al., Understanding the nonlinear effects of the street canyon characteristics on human perceptions with street view images. Ecological Indicators, 2023. 154: p. 110756. https://doi.org/10.1016/j.ecolind.2023.110756.
[35] Qiu W., et al., Subjective and objective measures of streetscape perceptions: Relationships with property value in Shanghai. Cities, 2023. 132: p. 104037. https://doi.org/10.1016/j.cities.2022.104037.
[36] Chen Z., et al., Using structural equation modeling to examine pathways between environmental characteristics and perceived restorativeness on public rooftop gardens in China. Frontiers in Public Health, 2022. 10: p. 801453. https://doi.org/10.3389/fpubh.2022.801453.
[37] Deng L., et al., Effects of integration between visual stimuli and auditory stimuli on restorative potential and aesthetic preference in urban green spaces. Urban Forestry & Urban Greening, 2020. 53: p. 126702. https://doi.org/10.1016/j.ufug.2020.126702.

[38] Jiang X., et al., Effects of virtual exposure to urban greenways on mental health. Frontiers in Psychiatry, 2024. 15: p. 1256897. https://doi.org/10.3389/fpsyt.2024.1256897.
[39] Chan S.H.M., et al., Nature in virtual reality improves mood and reduces stress: evidence from young adults and senior citizens. Virtual reality, 2023. 27(4): p. 3285-3300. https://doi.org/10.1007/s10055-021-00604-4.
[40] Reece R., et al., Exposure to green, blue and historic environments and mental well-being: a comparison between virtual reality head-mounted display and flat screen exposure. International journal of environmental research and public health, 2022. 19(15): p. 9457. https://doi.org/10.3390/ijerph19159457.